

N 7 3 3 2 6 1 7

**N A S A T E C H N I C A L
M E M O R A N D U M**

NASA TM X-71422

NASA TM X-71422

CASE FILE
COPY

INVESTIGATION OF MERCURY THRUSTER ISOLATORS

by Maris A. Mantenieks
Lewis Research Center
Cleveland, Ohio

TECHINICAL PAPER proposed for presentation at Tenth Electric Propulsion
Conference sponsored by the American Institute of Aeronautics and Astronautics
Lake Tahoe, Nevada, October 31-November 2, 1973

INVESTIGATION OF MERCURY THRUSTER ISOLATORS

Maris A. Mantenicks
Lewis Research Center
National Aeronautics and Space Administration
Cleveland, Ohio

Abstract

Mercury ion thruster isolator lifetime tests were performed using different isolator materials and geometries. Tests were performed with and without the flow of mercury through the isolators in an oil diffusion pumped vacuum facility and cryogenically pumped bell jar. The onset of leakage current in isolators tested occurred in time intervals ranging from a few hours to many hundreds of hours. In all cases, surface contamination was responsible for the onset of leakage current and subsequent isolator failure. Rate of increase of leakage current and the leakage current level increased approximately exponentially with isolator temperature. Careful attention to shielding techniques and the elimination of sources of metal oxides appear to have eliminated isolator failures as a thruster life limiting mechanism.

I. Introduction

Isolators are required on mercury ion thrusters to decouple the thruster high voltage from the propellant feed system. This requirement becomes especially desirable when multiple thruster applications are considered. The isolator must be able to withstand high voltage (~ 2 kV) with acceptably low electrical leakage currents. Studies have shown that isolators of both the segmented and tortuous path design can withstand the required thruster voltages. (1,2,3)

Isolator performance in thrusters has been inconsistent. Long lifetimes in small thrusters have been observed (4,5). However, leakage problems encountered earlier with the SERT II thruster isolator (6) have not been completely eliminated in the larger 30-cm thrusters which operate at higher temperatures.

There does exist some literature on the subject of leakage currents through and conductivity of insulator materials. These data are also inconsistent. The conductivity of aluminum oxide in vacuum and at high temperature has been observed to decrease with time in irradiation studies (7) and in short term tests. (8,9) In the latter two studies this effect was attributed to evaporation of surface impurities. Onset of leakage current in a 120-hr test was observed by Hartman. (10) Insulator leakage has also been observed in lifetime tests of high temperature ceramic thyratrons and voltage-regulator tubes. This leakage was attributed to sputtering. (11) Heater-cathode insulator failures have been reported in vacuum tube studies. (12,13) These failures were attributed to metal or metal oxide migration through porous ceramic.

The present study was undertaken to identify long term isolator failure mechanisms and develop an isolator for long term large thruster applications. Tests were conducted in bell jars with and without mercury flow through the isolator. Different isolator geometries, insulating materials, and heater and end cap materials were tested. The

effect of a diffusion pump oil environment on isolator performance was also observed.

II. Apparatus

Isolators

Figure 1 shows the general details of an isolator used with a mercury ion thruster. It consists of a cylindrical ceramic (high purity aluminum oxide) body with end caps usually made of Kovar or tantalum. The ceramic is metalized and the end caps are copper brazed to the metalized ceramic. To withstand the required thruster voltages (~ 2 kV), the isolator body has internal segments consisting of ceramic rings and very fine metal mesh screen. (2) Heaters are attached to the isolator to prevent mercury condensation during thruster startup. During normal steady state operation, the discharge plasma provides adequate heat flux to the isolator. In the bell jar isolator tests reported herein, heaters provided all the power required to reach the desired operating temperatures. Shields were used for some isolator tests to protect the isolator surface from ambient particle flux.

The isolators tested are described in Table I and shown in Figure 2. Isolators A and B are parts of a standard cathode-isolator-vaporizer (CIV) and main isolator-vaporizer (MIV) assemblies, respectively, fabricated by Hughes Research Laboratories. The CIV tests were run with a cathode discharge, whereas the MIV designs were tested with no flow.

Because it was found that isolators developed leakage current without the flow of mercury, isolators C and D (Fig. 2(c) and (d)) were fabricated without the internal structure of the standard isolators. This simplification expedited fabrication.

Isolator C (Fig. 2(c)) was fabricated from an aluminum oxide tube of unknown composition with TICUNI brazed tantalum end caps. (Inadvertently, braze containing silver was used as filler material following the initial brazing.) Isolator D (Fig. 2(d)) was similar to isolator C except Lucalox was used as the ceramic. No metalizing was applied to either of the two isolators before the brazing operation. Tantalum or Nichrome heaters were spotwelded on the end caps.

Isolators E and F (Fig. 2(e) and (f)), fabricated by Hughes Research Laboratories, were basically parts of a modified CIV assembly. The fins were made for the purpose of providing a large thermal gradient between the interior and exterior of the isolator to allow the surface of the isolator to run as cool as possible. Different configurations of heaters and shields, to be described later in more detail, were tested with these two isolators.

Isolator G (Fig. 2(g)) consisted of a modified CIV incorporating changes due to the observed results of the previous tests. The end caps, vaporizer, vaporizer heater, and the copper braze joint

were nickelplated. Shields made of nickel-plated stainless steel were attached to the isolator mechanically without the use of spotwelding. This CIV assembly was tested with an operating cathode with a solid barium impregnated insert

Iron-constantan thermocouples were attached to both end caps of all isolators except isolator A, test 1, where only the vaporizer temperature was measured.

Electrical System

An electric schematic of a typical isolator test including mercury flow, keeper and collector discharges is shown in Figure 3. Tests without mercury flow incorporated only two ac heater supplies with the high voltage applied across the isolator. In all cases the cathode end of the isolator was mounted on an electrical standoff and was held at ground potential. The opposite side was biased negatively by a high voltage dc power supply. This arrangement simulated the voltage gradient on a thruster.

The isolator current and high voltage were recorded on a strip chart recorder. Currents and voltages of various supplies were read on appropriate panel meters. Temperatures were read on panel meters.

Vacuum Facilities

All tests, except test 2 of isolator E, were conducted in 30-cm diameter ports on the 7.6 m x 18.3 m vacuum facility with diffusion pumps. A solid shield was installed to separate from the isolator, the keeper and collector discharge efflux and the flux from the large facility. The pressure in the port with an operating discharge was approximately 5×10^{-5} torr.

Test 2 of isolator E was conducted in a cryogenically pumped bell jar. No oil roughing or diffusion pumps were used, thereby providing an oil-free environment. The pressure in the bell jar was approximately 1.0×10^{-6} torr during the test.

III. Results

A brief summary of the results of the various tests appears in Table II. In this table isolator operating conditions (temperature, applied high voltage, and discharge currents, if used) are presented. Also, the initial isolator current at operating temperature and voltage is shown as well as the time of the onset of leakage current. Activation energies, as determined from the slope of the log of conductivity as a function of the reciprocal of the temperature curve, at various leakage current levels are also presented. The results of each test will now be discussed in more detail.

Isolator A

Test 1 As already described, isolator A was part of a standard 30-cm thruster CIV assembly. The cathode was run with a discharge current of 10A and discharge voltage of about 40 V. Initial isolator current at 1300 V and vaporizer temperature (very near the isolator temperature) of 330°C was approximately $2 \mu\text{A}$. The onset of leakage current,

taken to be the point at which the rate of increase with time increased rapidly, occurred after approximately 130 hours (Fig. 4(a)). After the onset of leakage current, the rate of increase of the leakage current at 330°C was approximately $1.1 \mu\text{A/hr}$ and the rate increased to $2.7 \mu\text{A/hr}$ at an isolator temperature of 345°C (Fig. 5). The plot of the log of leakage current as a function of the reciprocal of the temperature is seen in Figure 6. It is noted that the curve has essentially two slopes from which activation energies of the conducting layer may be calculated.

The voltage-current characteristics for this isolator were observed to be ohmic.

After the test was terminated, the shield was removed and the ceramic examined. The surface appeared to have a slight grayish color and the shield showed some discoloration but no obvious signs of a problem were observed. The ceramic surface was cleaned by aluminum oxide bead blasting and after reinstallation the leakage current returned very nearly to the initial current value of test 1. The return of leakage current to its base level after surface cleaning was true of all isolators tested, which indicated that the leakage current was an outside surface phenomenon.

Test 2 It was thought that the original shielding may not have been adequate to protect the isolator from the ambient particle flux and therefore another shield was added. A thin stainless steel shield was spotwelded to the end cap on the vaporizer side of the isolator. The original shield was then spotwelded back to its original position. The onset of Leakage current occurred within several hours.

Test 3 Due to the short term failure of the double shielded isolator, a test was run with all shields removed. As usual, the isolator surface was bead blasted previous to the test. In the cleaning process, however, it was possible that some of the nickel-plating on the Kovar end caps was removed. In this test the initial leakage current was higher than on previous tests, but the time to the onset of leakage current was longer (210 hrs) than for the previous two tests (Fig. 4(a)). Sudden increases of leakage current, were observed after vacuum tank shutdowns.

Isolator B

Test 1 During thruster operation it had been observed that MIV's did not suffer the leakage problem encountered in CIV's. Therefore, it was decided to test a MIV, but at a higher temperature and higher voltages than typical of thruster operation. No mercury flow was used for all three MIV tests. The isolator began to fail at about 220 hours (Fig. 4(a)).

Test 2 At this point it was thought that contamination of the aluminum oxide may have occurred during the sintering process of the ceramic. Therefore, it was decided to grind off a layer of the outside surface of the ceramic. The shield was not replaced for this test. The isolator began to fail after approximately 350 hours. It should be noted that because of the absence of the shield the isolator ran cooler during this test than in the previous test.

Test 3. To test the possibility that the diffusion pump environment was a possible cause for isolator failure a drop of diffusion pump oil was placed directly on the isolator surface. The initial isolator current was $0.4 \mu\text{A}$, considerably higher than on the previous two tests and it also began to fail sooner (190 hrs) than the previous two tests (Fig. 4(a)).

Isolator C

This isolator was fabricated in order to test isolator material effects on isolator leakage. As already described, stock aluminum oxide was used, which was probably of low purity. The Lifetime history of the isolator is shown in Fig. 4(b). The applied isolator voltage was raised from 2 kV to 4 kV after 380 hours of operation during which time the isolator current was constant. After 500 hours of operation the isolator was removed from the vacuum facility and inspected. It was found that a film $\sim 1.3 \text{ cm}$ long ($1/4$ of the total length of the ceramic) had appeared on the negative high voltage side of the isolator. The test was resumed and the onset of leakage current was observed at approximately 600 hours. The isolator again was inspected after 830 hours at a leakage current level of $5 \mu\text{A}$. The black film of contamination had progressed to about 2.5 cm ($1/2$ of the total ceramic length). Inspections of the isolator at 1020 hours (leakage current at $13.5 \mu\text{A}$) and later at the end of the test (leakage current at $385 \mu\text{A}$) revealed that the black discoloration had not progressed any further. This isolator exhibited a non-ohmic volt-ampere characteristic at high voltages (Fig. 7). The characteristic became ohmic, however, as the level of leakage current increased.

The activation energy of the isolator material before the onset of leakage current was 0.63 eV . However, after the onset of leakage current, the activation energy decreased and was comparable to those of other isolators ($0.15 - 0.30 \text{ eV}$).

Spectrographic analysis of the black discoloration disclosed that both sodium and silver were present in the film.

Isolator D

Test 1. Isolator D was also fabricated to study the effects of different isolator materials on isolator leakage. The configuration of the isolator was the same as isolator C except Lucalox was used as the ceramic body. A shield made of aluminum oxide tubing was placed concentrically over the isolator surface. The isolator failed within hours.

Test 2. The ceramic shield was removed, tantalum heaters replaced the Nichrome heaters, and a tantalum disk shield was attached to each end cap (Fig. 2(d)). The shields were to protect the isolator surface from the hot heater surfaces. Also the high voltage was reduced from 4 kV to 2 kV.

Initial isolator current at 410°C and 2 kV was $3.2 \mu\text{A}$. After approximately 700 hours the leakage current had dropped slowly to $1.5 \mu\text{A}$ before starting slowly to increase (Fig. 4(b)). The increase was not the typical exponential behavior observed in the previously tested isolators. Sev-

eral increases in leakage current appear to be due to vacuum facility shutdowns. After accumulating over 2200 hours, the leakage current is only about $11 \mu\text{A}$. The test is still in progress.

Isolator E

Test 1. The isolator with the ground off outer surface was outgassed at 500°C and tested at 460°C . The isolator began to fail only after approximately 6 hours (Fig. 4(a)). It was observed that a leakage path existed on both the outer and inner surfaces of the hollow isolator. Examination of the heaters after the test revealed that the stainless steel sheath of the heater as well as the Kovar end caps and shields had oxidized.

Test 2. In order to test the isolator in an oil-free environment, isolator E was cleaned and installed in a bell jar cryogenically pumped with liquid helium. The Nichrome heaters were replaced with tantalum heaters. This isolator began to fail in approximately 175 hours.

Isolator F

Test 1. Isolator F (Fig. 2(b)), similar to isolator E, was tested with tantalum heaters in the large oil diffusion pumped vacuum facility. After 220 hours of steady operation an inadvertent test shutdown resulted in oxidation of the tantalum heaters. The isolator failed catastrophically after resuming the test with the oxidized heaters.

Test 2. The isolator was cleaned by glass bead blasting and new tantalum heaters were installed. Also thin tantalum shields were spot-welded on the isolator end caps to protect the ceramic surface from the hot heater surfaces and from the ambient flux. The isolator failed within very few hours.

Isolator G

Isolator G, a CIV assembly (Fig. 2(g)), was fabricated keeping in mind the suspected failure modes on all the previous tests (see Discussion). In order to reduce oxidation of hot metal surfaces, the end caps, vaporizer, and shields were nickel-plated. The shields were attached mechanically, instead of employing the spotwelding technique used before. The initial current at 330°C and 1200 volts was $1.3 \mu\text{A}$. During 985 hours no onset of leakage current has been observed (as defined before). There has been a small incremental increase during this time up to $3.6 \mu\text{A}$. It has been noted that the increases were almost always associated with the startup of thrusters at other ports in the facility. The test is still in progress.

IV. Discussion

This section will discuss the variation of the leakage current with time and as a function of several parameters. A discussion of possible sources of isolator failure observed in the tests will be presented.

Leakage Current as a Function of Time

Figures 4(a) and (b) show leakage current as a function of time for many of the isolators tested. At this writing isolators D and G are still in test.

It is convenient to discuss separately the observed short and long term effects

Immediate failures were observed in test 1 of isolator A, test 1 of isolator D, and test 2 of isolator F. All three tests included the procedure of spotwelding shields on the isolators. It was concluded that spotwelding may be detrimental to isolator performance in two ways. First, metal evaporated during the spotwelding procedure may contaminate the isolator surface. Second, the localized heating during the spotwelding may have oxidized the shields and/or end caps and also destroyed the nickel-plating on the end caps. As will be discussed later, either phenomena could lead to isolator failure. Spotwelding was therefore eliminated in fabrication of isolator G, which at this writing has accumulated 985 hours of operation without the onset of leakage current.

Another short term failure occurred in test 1 with isolator E. During this test the isolator was outgassed at 500°C which required heater temperatures in excess of 800°C. Oxidation of heaters and end caps occurred, which was felt to be the cause of the immediate failure. The catastrophic failure in test 1 of isolator F was also determined to have occurred due to oxidation which took place after an inadvertent pressure rise in the bell jar.

Isolators that exhibited long lifetimes showed several trends of isolator current with time. Typically at test start, the leakage current would first increase with increasing isolator temperature and then slowly decrease for a few hours as the isolator reached thermal equilibrium. The short term decrease in leakage current may have been caused by evaporation of surface impurities.⁽⁹⁾ Long term decreases in isolator current for time periods of several hundred hours were observed in test 1 of isolator C and test 2 of isolator D. This long term behavior is not presently understood.

The base level of isolator current, after initial transient behavior, varied from about 0.1 μ A to 6.0 μ A dependent on isolator type and history. It is presently felt that the major share of the baseline leakage was across the surface rather than through the bulk ceramic. Estimates of the bulk leakage are obscured by the large range quoted for the conductivity of aluminum oxide in the literature.⁽⁹⁾ Use of the larger literature values of bulk conductivity led to estimates of bulk currents less than 0.1 μ A at test conditions. It was also determined that the presence of mercury flow and a cathode discharge always contributed less than 0.5 μ A to the baseline leakage current.

After the establishment of a baseline leakage current, all isolators except test 2 of isolator D and isolator G suffered a rapid increase in leakage current at time periods ranging from about 100 to 600 hours. The increase of leakage current with time was typically first exponential and generally then became linear. After this onset of current, the isolator was considered to have failed.

As already mentioned, bead blasting of the ceramic surfaces exposed to vacuum always restored the leakage current to a low value. This indicated that the leakage current associated with the failure was always a surface leakage phenomenon.

Sources of Surface Contamination

Because the prime failure mechanism has been associated with leakage across the isolator surface, possible sources of surface contamination and tests which are relevant to the identification of such sources are discussed separately below.

Vacuum Facility Environment Test 3 of isolator B and test 2 with isolator E were addressed specifically to the question of vacuum pump oil contamination of the isolators. Oil contamination of insulator surfaces has been observed in several experiments^(14,15,16) As previously mentioned, in the former test a drop of diffusion pump oil was placed directly on the ceramic surface and isolator B failed in 190 hours. Because this failure time was similar to failure time of the isolator in the previous test, the exact importance of the oil environment could not be specified at that time. Isolator E was then tested in a LiHe pumped, oil-free bell jar and failed in about the same time as similar units previously tested. The effects of vacuum pump oil were therefore eliminated as a primary source of surface contamination.

As has been mentioned, oxidation of isolator components has been identified with certain of the isolator short term failures. Because a partial pressure of oxygen always exists in any vacuum facility, it appeared desirable to provide protection against long term oxidation effects. To this end, all the metallic components of isolator G were nickelplated.

Ceramic Type Aluminum oxide of three levels of purity were used in the isolator tests. It is likely that the choice of insulator material did not strongly affect isolator lifetimes. Isolator C, which was made of stock grade aluminum oxide, performed in a fashion equivalent to most of the isolators which used a higher purity insulator. Also, isolator D failed immediately in test 1 but ran for an extended time period in test 2. It should be mentioned, however, that in some tests surface contamination of low purity aluminum oxides has been observed after vacuum firing.⁽¹⁷⁾

Sputtering Ion sputtering could lead to the deposition of contaminants on the ceramic surface. Ions could be made available either via plasma leakage from the cathode discharge, if present, or as a product of microdischarges directly across the isolator. The former source of ions is not considered likely as isolator A actually failed more quickly when doubly shielded than when no shields were present. The possibility of microdischarges cannot be completely discounted at this time. However, no evidence of pitting of metallic surfaces typical of sputtering damage was ever observed on any isolator after failure.

Chemical Reactions A brief search was made to determine if chemical interactions with the bulk ceramic material were of importance. In general, the temperatures required for significant chemical effects are far in excess of the test temperature of isolators.⁽¹⁸⁾ It should be noted that in many cases, such as for chemisorption of H_2 or O_2 , the resistivity of aluminum oxide actually increases with increasing temperature⁽¹⁹⁾ in contrast to the observed behavior of isolators.

Evaporation from Isolator Components. As previously suggested, many of the long term failures are probably due to the evaporation and subsequent condensation upon the ceramic surface of metals and/or metal oxides. Steps were taken early in the program to eliminate elemental materials of high vapor pressure (such as cadmium, zinc, and materials containing these elements such as silver solder and solder flux). Following these steps long term isolator failures still occurred.

Details of the evaporation, deposition, and consequent electrical conductivity of thin metal-metal oxide films are complex^(20,21) especially in the presence of applied voltages where migration of mass can occur^(8,22). It is tentatively assumed herein that the primary source of the metal or metal oxide was evaporation of metallic oxides formed on the hotter parts of the isolator. This seems likely for several reasons: (1) The vapor pressure of the metals used appears to be too low to account for sufficient evaporated material to cause the observed failures, (2) The oxides of metals in some cases have vapor pressures many orders of magnitude larger than that of the base metal, and (3) Many of the physical trends of isolator leakage after a long term failure are very similar to the trends after the short term failures where the failure mechanism was almost certainly identified as metal oxide formation and deposition on the ceramic surface.

Evaporation of the metal oxide films can produce either the elements or the oxides themselves as the major vapor constituents^(20,23) and hence may result in either a metal and/or metal oxide film deposition upon a surface. It is interesting to note that the mass, or thickness, deposition of a vapor is not generally a linear function of time in the initial phases⁽²¹⁾ (Fig 8). In addition, as seen in Figure 9, the resistivity of thin metallic films is not generally linear with film thickness.⁽²⁴⁾ Although not certain, it is possible that a combination of these two phenomena may be responsible for the generally nonlinear onset of leakage current observed in the long term failures (Fig. 4).

It has also been determined that the conductivity of both semiconductive films⁽²¹⁾ and thin metallic films^(25,26) depends exponentially upon the reciprocal of temperature. The slope of the leakage current versus inverse temperature plotted on semilog paper is linear and yields the activation energy for the deposited material. In some cases with a semiconductive film, such as a metal oxide, two linear slopes occur which arise due to the effect of impurities. In addition, it has been found that the activation energy sometimes decreased with time (or increasing leakage current)⁽¹⁰⁾.

As mentioned previously, and shown in Figure 6, the functional dependence of leakage current on temperature was similar to that described above. In most CIV and MIV tests two linear slopes were found, which is suggestive of a semiconductive layer with impurities. However, in other isolator tests only one slope was present, which may indicate the presence of a thin metallic film. The strong dependence of activation energy upon such variables as thickness and impurities precluded identification of contaminant type by activation energy.

The rate of increase of isolator current was determined to rise rapidly with increasing temperature (Fig. 5). The data for isolators A and E on Figure 5 were obtained after the onset of leakage current had occurred. The exact reasons for the rate dependence on temperature is not known but it is probably due to both increased oxidation of hot surfaces and evaporation of such oxides at elevated temperature.

The volt-ampere characteristics of isolator C are shown in Figure 7 for three test times. As was typical of most isolators discussed herein, the leakage current was generally ohmic after the onset of leakage current. In some cases the isolators exhibited slight non-ohmic behavior early in a test (at low values of leakage current). The observed current-voltage plots are consistent with metal or metal oxide thin film characteristics.

Some evidence was obtained with isolators A and E which demonstrated that the rate of increase of leakage current increased with increasing voltage. Such data are difficult to obtain, however, due to the difficulty of maintaining a constant temperature in light of the strong dependence of isolator current on temperature. This evidence, along with the visual observations of isolator C mentioned previously, indicate that migration of impurities or possibly sputtering due to microdischarges could also have contributed to the increase of leakage current with time. The relative importance of these effects are, however, not known at this time.

V Conclusions

Isolators with various geometries and materials have been tested with and without mercury flow in vacuum facility environments with and without diffusion pump oil. The onset of leakage current in many isolators occurred from almost immediately to many hundreds of hours.

It was felt that some isolator failures were caused by isolator surface contamination during the spotwelding of shields on isolator end caps. Local oxidation and evaporation during spotwelding probably resulted in formation of a conductive film on the isolator surface. Inadvertent oxidation during facility shutdown also resulted in some short term isolator failures.

The long term failure mode was found also to be due to isolator surface contamination. The major source of contamination is felt to be due to evaporation of metals or metal oxides and consequent condensation of a conductive film on the ceramic surface. The rate of increase of leakage current and total leakage current increased approximately exponentially with isolator temperature.

Tests on an oil-free vacuum facility showed that the long term failure mechanism was not primarily due to the presence of vacuum pump oil.

Other possible failure mechanisms such as sputtering, chemical interactions, effects of bulk ceramic are considered to be of secondary importance for the tests presented herein.

An isolator, fabricated to eliminate contamination sources: did not show the onset of leakage

current typical of similar isolators tested The test of this isolator is still in progress.

VI. References

1. Nakanishi, S., "Experimental Investigation of a High-Voltage Isolation Device for Ion-Thruster Propellant Feed," TN D-3535, Aug. 1966, NASA.
2. King, H. J., Poeschel, R. L., Schnelker, D. E., Herron, B. G. and Collett, C. R., "Low Voltage 30 Cm Ion Thruster, Final Report," Feb. 1972, NASA.
3. Eye, J. W., "Component Development for a 10-Cm Mercury Ion Thruster," AIAA Paper 72-487, Bethesda, Maryland, 1972
4. Nakanishi, S., "Durability Tests of a Five-Centimeter Diameter Ion Thruster System," AIAA Paper 72-1151, New Orleans, La., 1972
5. Power, J. L., "Sputter Erosion and Depletion in the Discharge Chamber of a Small Mercury Ion Thruster," AIAA 10th Propulsion Conf, Nov 1973.
6. Byers, D. C. and Staggs, J. F., "SERT II Flight-Type Thruster System Performance," TM X-52520, 1969, NASA
7. Gregory, T. L., "Irradiation of High Purity Alumina," GEST-2101, June 1967, General Electric Co., Pleasanton, Calif.; also CR-72334, June 1967, NASA
8. Haveli, R. F. and Holtz, F. C., "High-Temperature Electrical Properties of Insulators and Their Compatibility with Refractory Metals," IITRI-B6016-17, Mar 1965, IIT Research Institute, Chicago, Ill.; also CR-54125, Mar 1965, NASA.
9. Cohen, J., "Electrical Conductivity of Alumin American Ceramic Society Bulletin, Vol. 38, No. 9, Sept. 1959, pp. 441-446
10. Hartmann, W., "Elektrische Untersuchungen an Oxydischen Halbleitern," Zeitschrift fuer Physik, Vol. 102, No. 11/12, 1936, pp. 709-733.
11. Jones, N. D., "Development and Endurance Testing of High-Temperature Ceramic Voltage-Regulator Tubes," CR-1813, Apr. 1971, NASA.
12. Noelcke, C. L., "Deterioration Mechanisms in Electron Tubes," Monograph No. 6, Nov 1958, ARINC Research Corp., Washington, D.C
13. Carroll, P. E., Cohen, J., Florio, J. V. and Wilson, A. L., "Heater-Cathode Investigation," Report No. YP56(B7-3028-1), June 1956, Sylvania Electric Products, Inc., Kew Gardens, New York.
14. Rosenbury, F., "Handbook of Electron Tube and Vacuum Techniques," Addison-Wesley Pub., Massachusetts, 1965.
15. Cleaver, J. S. and Fiveash, P. N., "A Study of Some Diffusion Pump Oils Using a Six-Inch Radius 60° Sector Field Mass Spectrometer," Vacuum, Vol. 20, No. 2, Feb 1970, pp. 49-54.
16. Ennos, A. E., "The Origin of Specimen Contamination in the Electron Microscope," British Journal of Applied Physics, Vol. 4, No. 4, Apr. 1953, pp. 101-106.
17. Literat, L., "New Data on Nonstoichiometric Alumina-Isothermic Variations in Electrical Conductivity as a Function of Oxygen Pressure," Cluj, Institutul Politehnic, Buletinul Stiintific, No. 7, 1964, (NASA-TT-F-9488), pp. 87-93.
18. Ryskewitch, E., "Oxide Ceramics: Physical Chemistry and Technology," Academic Press, New York, 1960.
19. Khoobiar, S., Carter, J. L. and Lucchesi, P. J., "Electronic Properties of Aluminum Oxide and the Chemisorption of Water, Hydrogen, and Oxygen," Journal of Physical Chemistry, Vol. 72, No. 5, May 1968 pp. 1682-1688.
20. Margrave, J. L., ed., "The Characterization of High-Temperature Vapors," Wiley, New York, 1967
21. Maissel, L. I. and Glang, R., eds., "Handbook of Thin Film Technology," McGraw Hill, New York, 1970.
22. Chaikin, S. W., Jarney, J., Church, F. M. and McClelland, C. W., "Silver Migration and Printed Wiring," Industrial and Engineering Chemistry, Vol. 51, No. 3, March 1959, pp. 299-304.
23. Kohl, F. J. and Stearns, C. A., "Oxidation/Vaporization of Silicide Coated Columbium Base Alloys," TM X-67980, Dec. 1971, NASA
24. Holland, L., "Vacuum Deposition of Thin Films," Wiley, New York, 1956.
25. Neugebauer, A. C. and Webb, M. B., "Electrical Conduction Mechanism in Ultrathin, Evaporated Metal Films," Journal of Applied Physics, Vol. 33, No. 1, Jan. 1962, pp. 74-82
26. Hill, R. M., "Transport Phenomena on Thin Films," Thin Solid Films, Vol. 12, 1972, pp. 367-381.

TABLE I - DESCRIPTION OF TESTED ISOLATORS

Isolator	Insulator material	End cap material	Ceramic-metal braze	Metal-lizing	Heater material	Isolator shields	Test facility
A (std. CIV) Test 1 Test 2 Test 3	99.8% Al ₂ O ₃	Ni-plated Kovar	Cu	Mo-Mn	See Ref 2	Stainless steel Original Double stain- less steel None	Diffusion pump
B (Std. MIV) Test 1 Test 2 Test 3	"			"	Nichrome	Stainless steel Original None	
C Test 1	Al ₂ O ₃ Unknown purity	Ta	TiCUNI	None	"		
		"	"	"	" Ta	Ceramic Ta	"
		Ni-plated Kovar	Cu	Mo-Mn	Nichrome	Stainless steel None	" Cryogenic pump
Test 2					"	None Ta	Diffusion pump
G (modified std. CIV) Test 1	"	"	"	"	See isolator A	Ni-Plated stain- less steel	"

TABLE II - ISOLATOR OPERATING CONDITIONS AND TEST RESULTS

Isolator	Temperature, °C	Initial (hot) current, μ A	Time of onset of leakage current	Applied voltage	Mercury flow or discharge	Activation energy at leakage current level	
						eV	μ A
A Test 1 Test 2 Test 3	330, 345 350 350, 370	2.0 4.0 6.0	130 Immediate 210	1300 1300 1300	10 A " "	0.19, 13 14, 12 15, 12 13	80 350 350 500
B Test 1 Test 2 Test 3	375 330 330	0.1 1 4	220 350 190	1700, 4000 4000 4000	None " "	0.26 42, 22 32	15 12 15
C Test 1	405	0.3	580	1200, 4000	"	0.63 .31	3 5.1
D Test 1 Test 2	405 410	4.0 3.0	Immediate Test in progress	4000 2000	" "	0.21	85
E Test 1 Test 2	460 385	0.1 .25	6 175	2000 2000	" "	0.22 .31	70 4
F Test 1 Test 2	420 440	3 9.0	220 Immediate	2000 1000	" "	0.17	0.17
G Test 1	330	1.5	Test in progress	1200	10 A	0.18, .06	2.5

*Activation energy measured before onset of leakage current

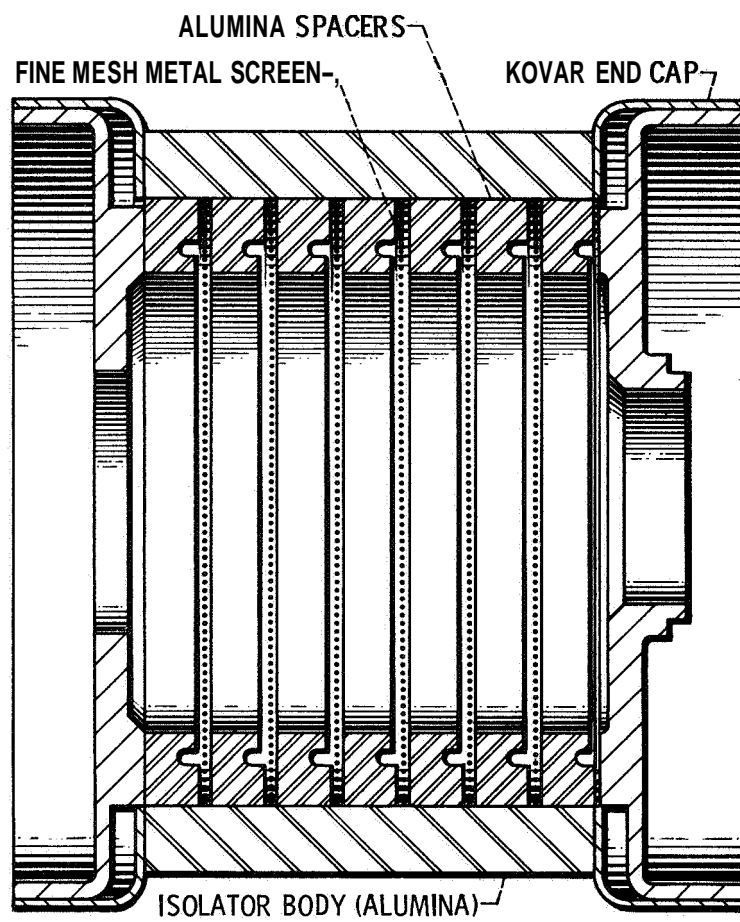
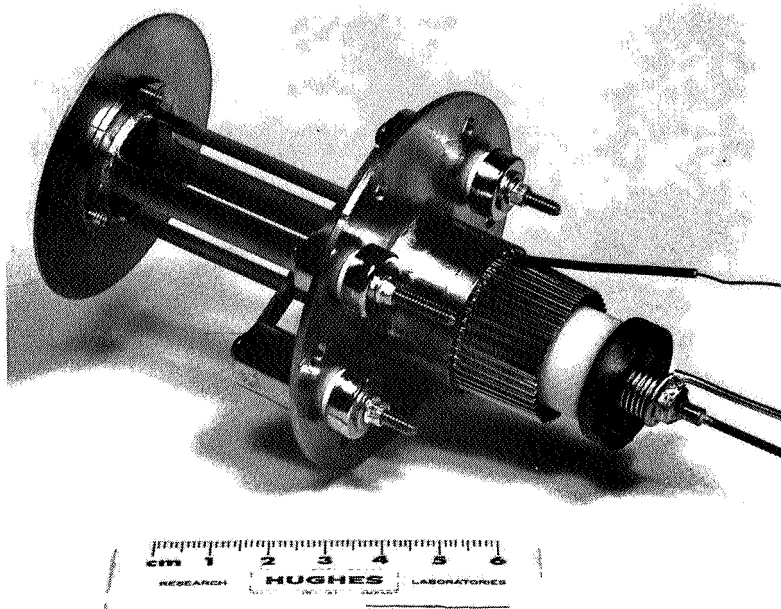
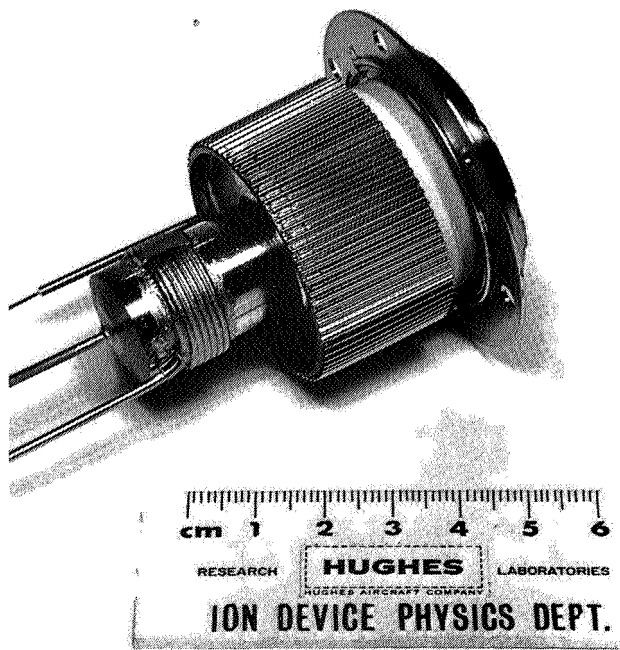


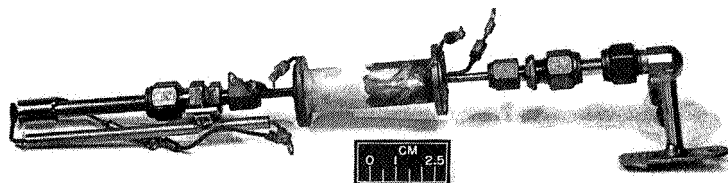
Figure 1. -Typical HG ion thruster segmented isolator (ref. 2)



(a) ISOLATOR A (CIV).



(b) ISOLATOR B (MIV).

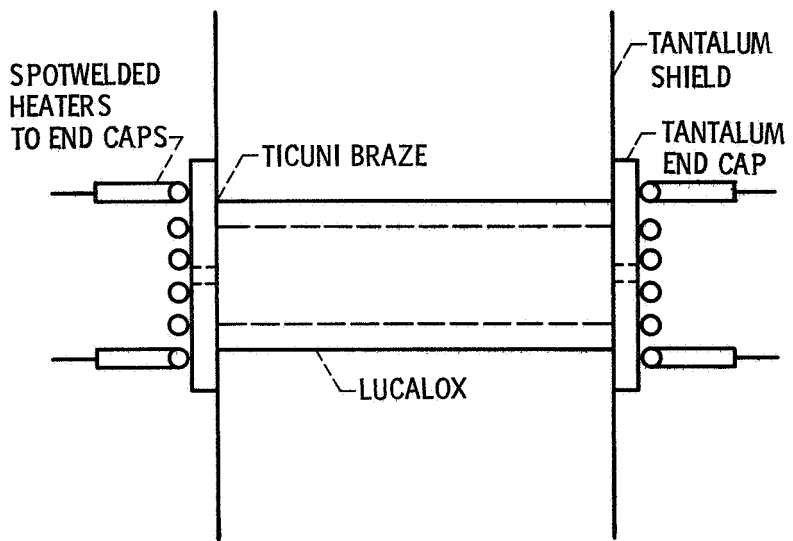


(c) ISOLATOR C.

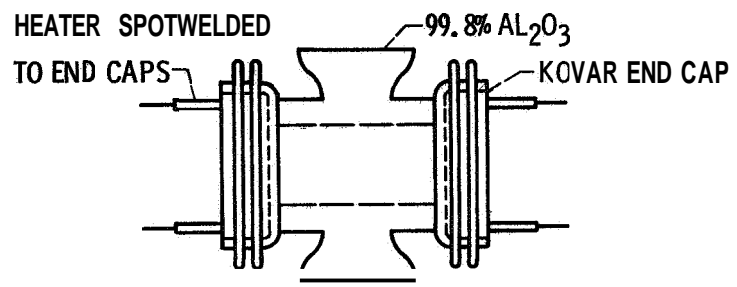
Figure 2. - Isolator configurations.

C-73-2071

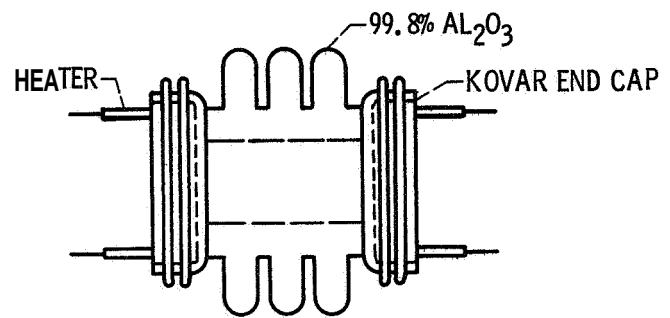
E-7664



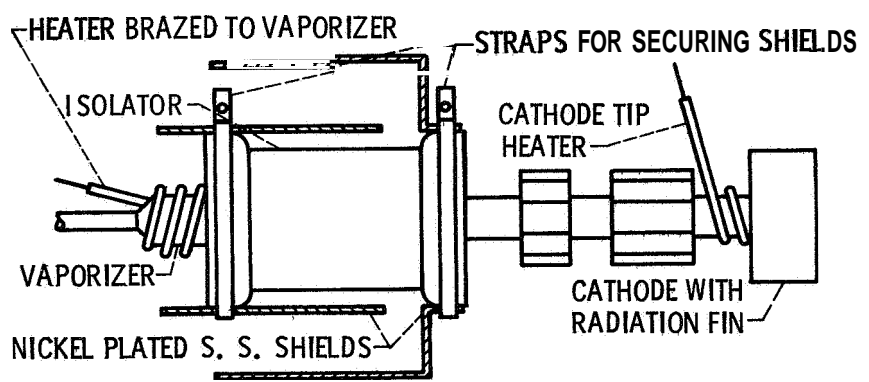
(d) ISOLATOR D



(e) ISOLATOR E



(f) ISOLATOR F



(g) ISOLATOR G (CIV)

Figure 2 - Concluded. Isolator configurations.

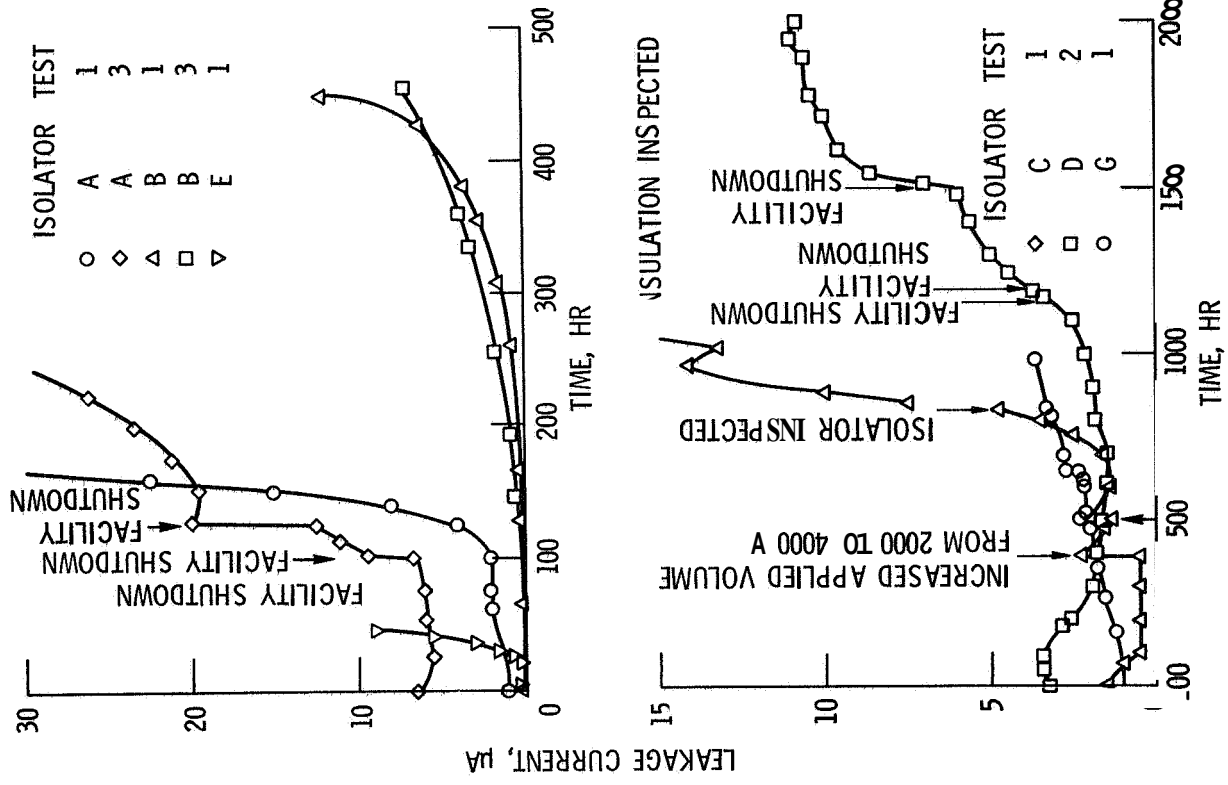


Figure 4. - Leakage current as a function of time.

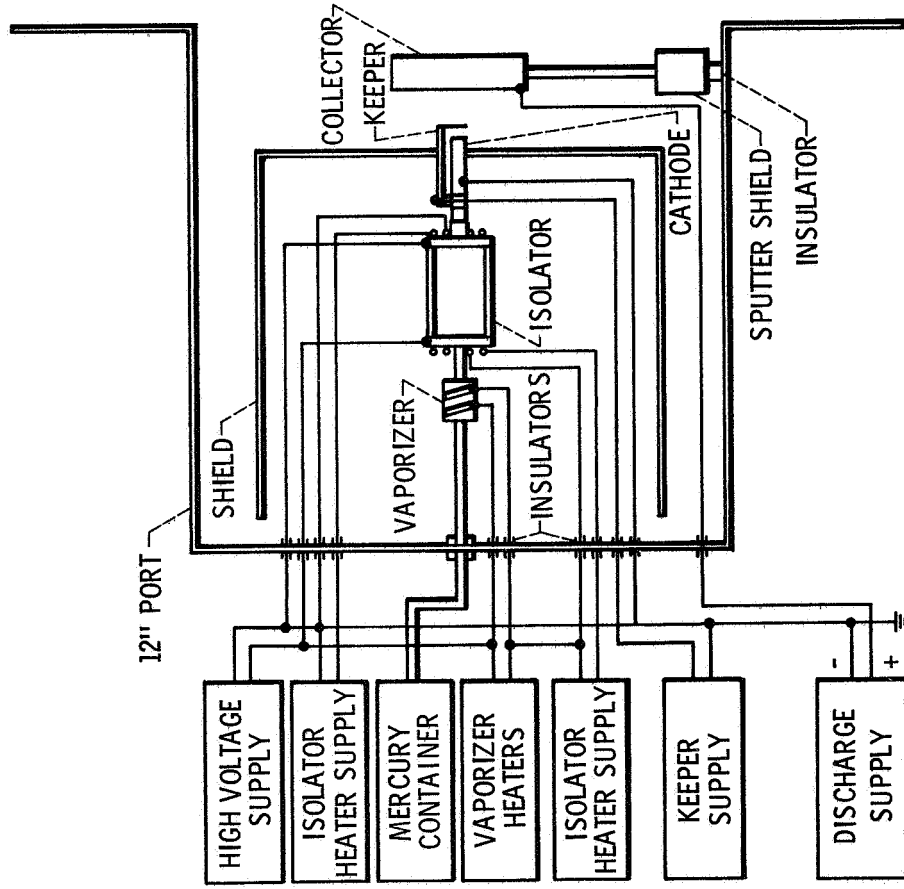


Figure 3. - Schematic of an isolator test with an operating cathode.

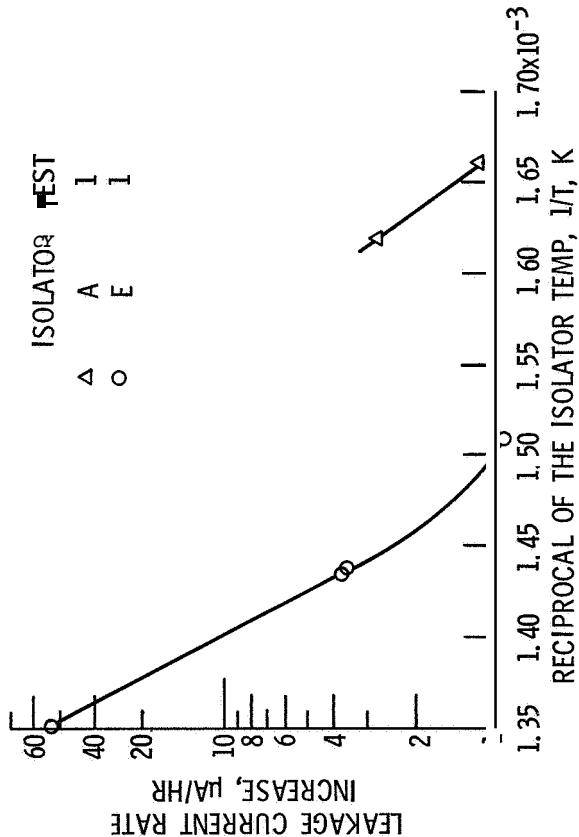


Figure 5. - Leakage current rate increase as a function of the reciprocal of the temperature.

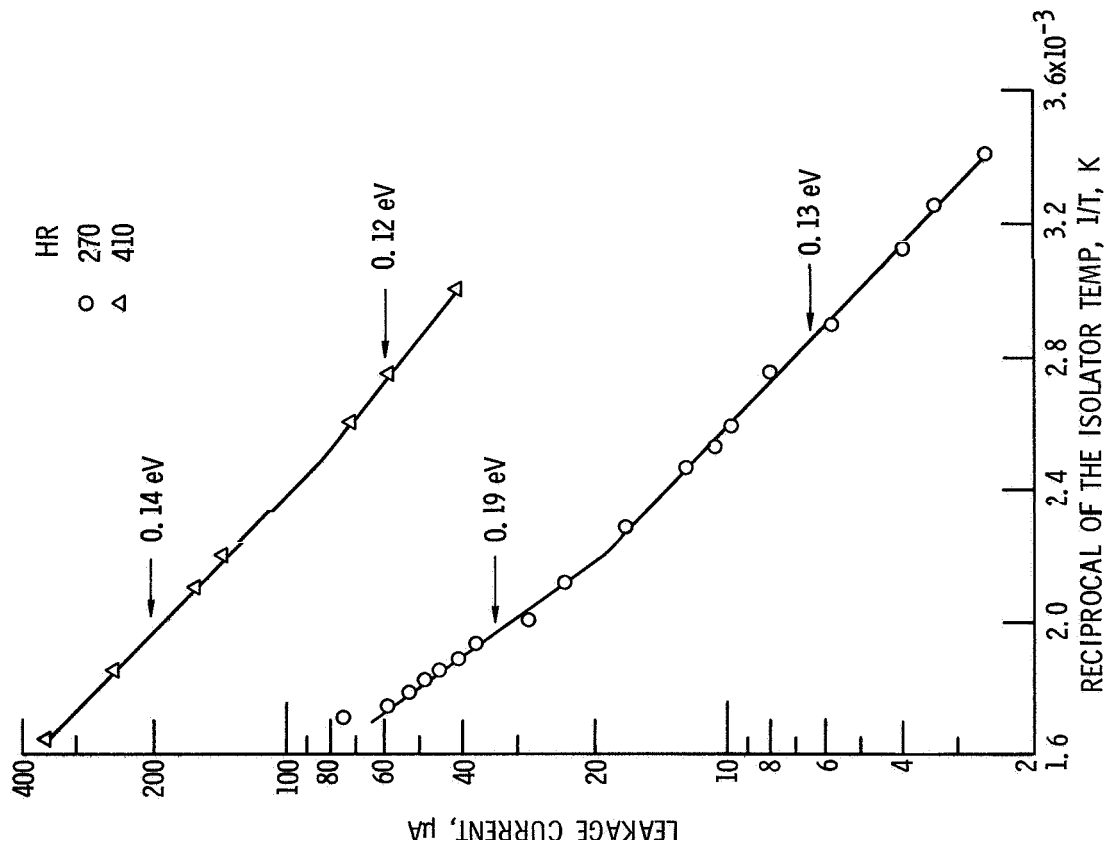


Figure 6. - Leakage current as a function of the reciprocal of the temperature of isolator A - test 1.

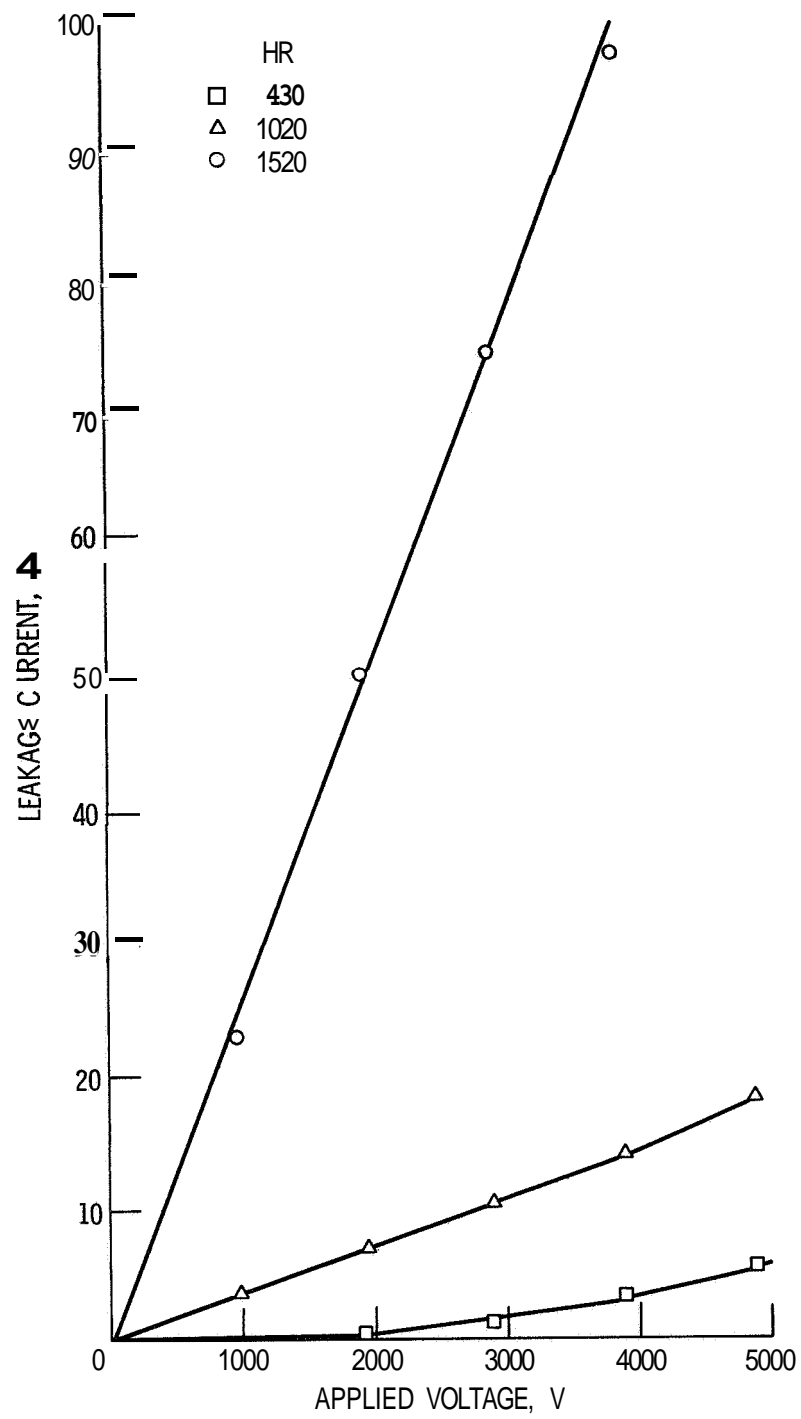


Figure 7. - Current-voltage characteristics of isolator C

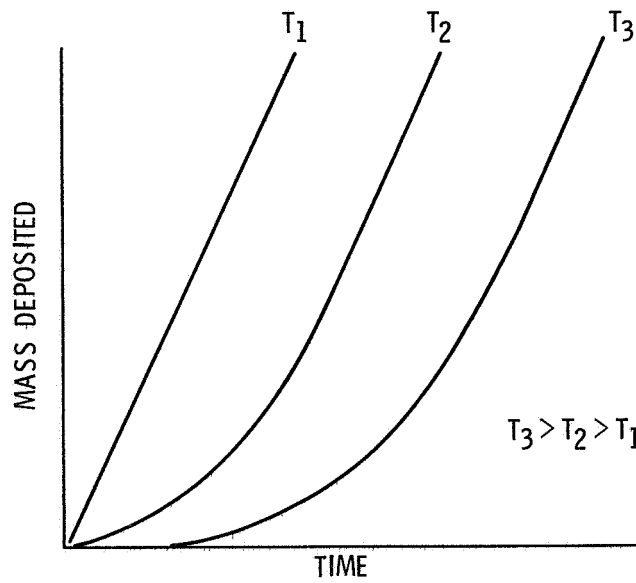


Figure 8. - Condensed mass deposited vs time at various substrate temperatures (ref 21).

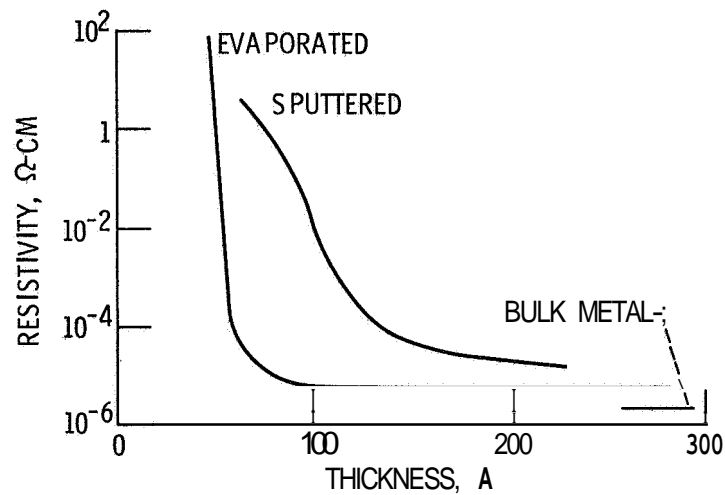


Figure 9. - Resistivity of sputtered and rapidly evaporated (2 sec) silver films as a function of thickness (ref. 24).